CHEMISTRY
A EUROPEAN JOURNAL

FULL PAPER

DOI: 10.1002/chem.201200737

Paramagnetic ^{19}F Chemical Shift Probes that Respond Selectively to Calcium or Citrate Levels and Signal Ester Hydrolysis

Peter Harvey, Kirsten H. Chalmers, Elena De Luca, Anurag Mishra,* and David Parker*[a]

Abstract: Paramagnetic magnetic resonance chemical shift probes containing a proximal CF_3 group have been characterised. Different systems have been created that report reversible changes in calcium ion concentrations in the millimolar regime, signal the presence of citrate selectively in competitive aqueous media and allow the monitoring of remote ester/amide hydrolysis in relayed, irreversible transformations. Chemical shift non-equivalence is amplified by the presence of the proximate lanthanide ion, with a mean separation between the CF_3 group and the metal ion of 6.4 Å found for a thulium complex, in an X-ray structure of the metal complex aqua adduct. The enhanced rate of longitudinal relaxation of the ^{19}F nucleus allows faster data acquisition.

Keywords: calcium · fluorine · lanthanides · magnetic resonance · paramagnetism

Introduction

Magnetic resonance methods have become pre-eminent in modern structural analysis because of the sensitivity of the observed chemical shift to molecular environment. In this respect, ^{19}F NMR spectroscopy studies with fluorinated probes offer considerable scope, as not only does this nucleus have a high receptivity (83% of ^{1}H) and Larmor frequency (376 MHz at 9.4 T), but also the chemical shift range is typically an order of magnitude greater than for ^{1}H NMR spectroscopy.[1] The acquisition of sufficient signal intensity in a short time-period remains a limiting feature of NMR spectroscopy and magnetic resonance imaging studies. This limitation can be obviated to a degree, by increasing the rate of relaxation of the observed nucleus, following introduction of a paramagnetic centre close to the nucleus being observed.[2–4] The steep distance dependence (r^{-6}) of the electron–nuclear dipolar interaction primarily determines the nuclear spin relaxation rates, R_1 and R_2. At very short distances, line-broadening is severe and limits spectroscopic studies particularly; at larger distances the increase in R_1 is less than an order of magnitude and any sensitivity gain arising from shorter acquisition times is reduced. A balance needs to be struck, striving also to minimise the R_2/R_1 ratio.

These issues have been addressed recently in the design of several paramagnetic lanthanide(III) complexes in which a homotopic CF_3 group is placed between 4.5 and 7.5 Å from the metal ion.[2–4] Sensitivity gains over diamagnetic controls in spectroscopy are of the order of a factor of 12,[3,4] and the use of zero echo time pulse sequences can increase sensitivity for imaging by a factor of about 25.[4c]

The broad chemical shift range of ^{19}F NMR spectroscopy prompted its early application in metabolism studies[5] of fluorinated drugs, as well as stimulating the development of responsive chemical shift probes.[1a,c,2] In each case, the observed shift most commonly reported an irreversible chemical transformation of the fluorinated probe, including those induced by enzymatic catalysis.[6] Examples have also been described in which reversible calcium binding to a fluorinated analogue of BAPTA[1d] was signalled by a change in the chemical shift of an aryl F label. However, the dissociation constant for calcium binding was in the micromolar range and hence beyond the normal sensitivity range of most magnetic resonance experiments.

When the fluorine label in a putative probe is close to a lanthanide ion within the same molecule, the pseudo-contact shift amplifies chemical shift differences between probe species. The dipolar shift induced (δ_p), varies as a function of the geometric coordinates of the ^{19}F nucleus with respect to the principal axis, as well as the local coordination environment of the Ln^{3+} ion. This is commonly expressed, for systems approximating to cubic symmetry, as [Eq. (1)]):

$$\delta p = C_D \frac{\beta^2}{60(kT)^2} \frac{(3\cos^2\theta - 1)}{r^3} B_2^0 \qquad (1)$$

where the geometric term includes the distance, r, between the probe nucleus and the metal ion and the angle, θ, defined with respect to the principal axis; β is the Bohr magneton, C_D is the Bleaney constant for the given Ln^{3+} ion and B_2^0 is a second-order crystal field coefficient that is strongly

[a] P. Harvey, Dr. K. H. Chalmers, Dr. E. De Luca, Dr. A. Mishra, Prof. D. Parker
Department of Chemistry, Durham University
South Road, Durham DH1 3LE (UK)
E-mail: anurag.mishra@durham.ac.uk
david.parker@durham.ac.uk

Supporting information for this article is available on the WWW under http://dx.doi.org/10.1002/chem.201200737.

dependent on the Ln^{3+} coordination environment.[7] It should be remembered that this shift effect does not apply to Gd^{3+} complexes, as the magnetic susceptibility tensor is nearly isotropic, due to the absence of orbital degeneracy. For the later Ln^{3+} ions (Tb, Dy, Ho, Er, Tm, Yb) the pseudo-contact shift variation therefore allows a general means of tracking changes in probe geometry (i.e., configuration or conformation) or metal ion speciation, by using NMR spectroscopy or chemical shift imaging.

Chemical shift probe design criteria: Two different cases can be considered for probe design, depending upon whether there is an irreversible transformation of the probe or a reversible change in its structure. In each case, it is highly desirable that the polar coordinates of the CF_3 reporter group do not change too much, so that the R_1 and R_2 parameters are minimally perturbed. In this way, standard pulse sequences can be employed throughout the monitoring process. A direct consequence of this strategy is that the fluorinated label should be maintained at a fixed distance from the Ln^{3+} ion. This approach may be contrasted with that adopted by Mizukami based on abrupt changes in line-broadening.[6e,f] Irreversible cleavage of a ^{19}F labeled peptide conjugate linked to a Gd complex was catalysed by an enzyme, and led to the formation of fragments where the Gd complex moiety was separated from the ^{19}F labeled entity. The removal of the proximate Gd moiety, that caused the initial ^{19}F signal to be very broad and difficult to observe, allowed the appearance of the diamagnetic 19F labeled fragment to be monitored. No change of chemical shift accompanied this process and the final species observed had a slow rate of relaxation.

In the first case, the irreversible transformation can be a functional group transformation of the ligand, for example, an amide or ester hydrolysis. Judicious positioning of the CF_3 label allows the perturbation in local electron density to be signalled by variation in δ_F. In the second case, a reversible interaction of the probe can occur either at the metal centre—for example, displacing a weakly bound ligand donor group or a solvent molecule—or at the ligand, or indeed at both sites simultaneously. The change in the local ligand field causes a variation in B_2^0 and this change is reported as a shift of δ_F [Eq. (1)].

Here, we report paramagnetic fluorinated magnetic resonance probes that have been designed with these criteria in mind. We establish these principles in three systems: the first reports a variation in calcium ion concentrations in the millimolar regime; the second signals the presence of citrate in competitive aqueous media; the third indicates ester/amide hydrolysis in a relayed, irreversible transformation. For the calcium probe example, we have modified the approach used recently in the design of Ca^{2+} and Zn^{2+} responsive Gd complexes. These examples were based on a reversible change in metal ion hydration state, leading to a large change in the water proton relaxivity.[8–10]

In the target complex, $[Ln{\cdot}L^1]$, a CF_3 group is fixed in position within a strongly coordinated arylamide moiety

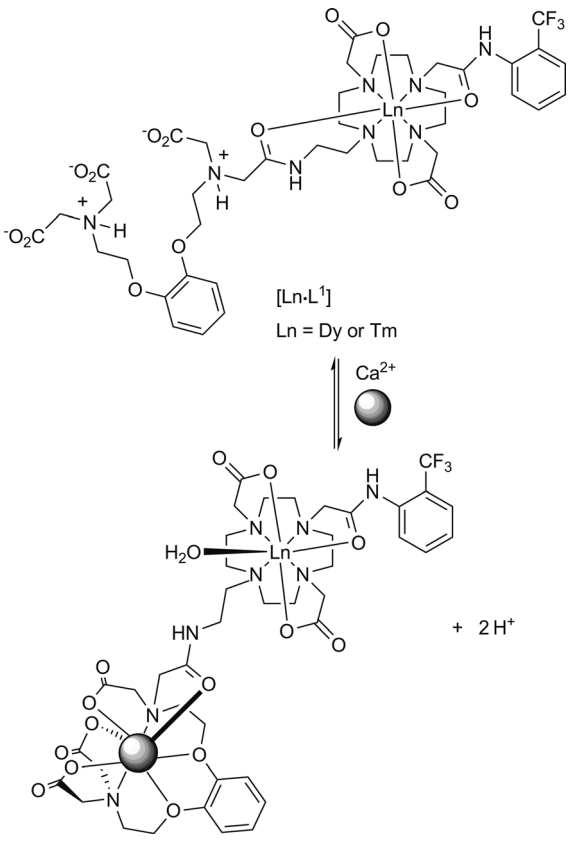

Scheme 1. Change in the lanthanide coordination environment induced by Ca^{2+} binding.

(Scheme 1). At the *trans*-position of the macrocyclic ring, a second amide carbonyl group forms part of a 7-ring chelate and is linked to a calcium selective binding site. This amide carbonyl is more weakly bound to the lanthanide ion[11] and when Ca^{2+} is present, the carbonyl oxygen prefers to bind to the Ca^{2+} ion and the Ln^{3+} coordination environment changes.[8,11] The coordination change at the metal centre is reported by the change in δ_F.

In the case of citrate signalling, most related reported probes have been based on the displacement of water at the metal centre in a coordinatively unsaturated complex of a heptadentate ligand. Typically, signal transduction with these probes has been based on the modulation of lanthanide luminescence. Systems have been created that allow the rapid and selective measurement of citrate in serum, urine or seminal fluids.[12–15] Here, the cationic monoamide complexes, $[Ln{\cdot}L^2]$ and $[Ln{\cdot}L^3]$, have been designed so that a coordinated water is displaced (Scheme 2) by the anion, whereas the CF_3 label remains in a constant relative position. Prototypical systems are reported here, in order to establish the principle of reporting reversible and selective anion binding by a change in δ_F.

Finally, examples are presented of the use of a change in δ_F, amplified by the presence of the proximate Ln^{3+} ion, to signal a remote functional group transformation. The sys-

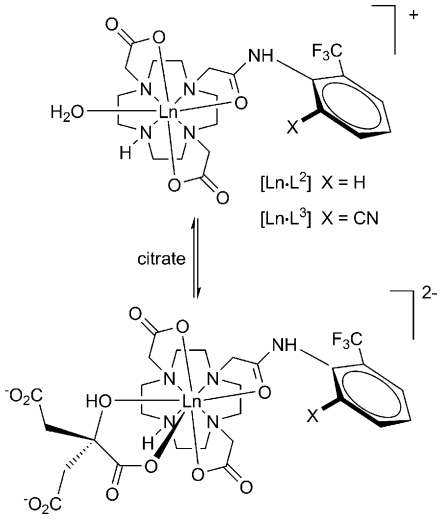

Scheme 2. Variation in lanthanide ion speciation following reversible citrate binding.

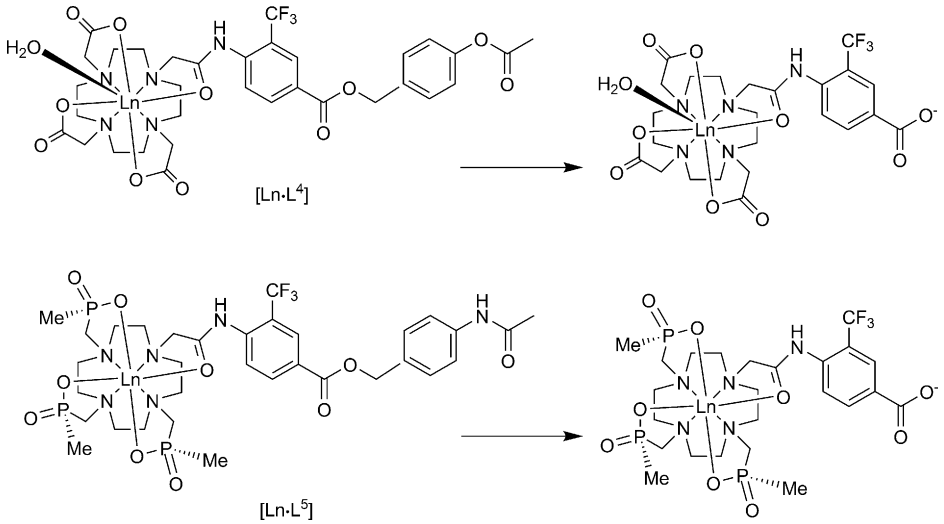

Scheme 3. Irreversible cleavage of the remote functional group signalled by a change in chemical shift of the reporting CF_3 group.

tems chosen also contain an integral CF_3 group in an amide-bound subunit, [Ln·L^4] and [Ln·L^5], in which the *para*-substituted aryl ester group is hydrolysed, following relayed cleavage[16,17] of the distal ester or amide group (Scheme 3).

Results and Discussion

Ligand and complex synthesis: The synthesis of ligand L^1 was undertaken by using a strategy that required formation of an amide bond between the Ca^{2+} binding site and the fluorinated paramagnetic reporter moiety (Scheme 4). Alkylation of the tertiary butyl ester of 1,7-bis(carboxymethyl)-1,4,7,10-tetraazacyclododecane (DO2A) by the α-chloroamides **1** or **2** yielded the corresponding monoamides **3** and **4**. Subsequent treatment of **3** with benzyl 2-bromoethylcarbamate in MeCN yielded the diamide **5**, from which the primary amine **6** was obtained following Pd-catalysed hydrogenolysis of the benzyl group. The acid, **7**, has previously been reported,[8] and was coupled with the amine **6**, by using standard carbodiimide methodology, to afford the protected amide, **8**. Following removal of the ester groups with TFA, the desired lanthanide complexes, [Ln·L^1], were formed by treatment with $LnCl_3 \cdot 6H_2O$ at pH 6.5. Any lanthanide ions that bound to the weaker Ca^{2+} binding site in L^1 were removed by treatment with Chelex^{TM} resin. The final complexes were purified by reverse phase HPLC, and gave rise to a single shifted ^{19}F NMR resonance, consistent with preferential formation of one main solution species. The lanthanide complexes of L^2 and L^3 were formed from **3** and **4** through a similar pathway (Scheme 4).

For the synthesis of the complexes [Ln·L^4] and [Ln·L^5], the ester groups were introduced in the final step, in each case (Scheme 5). The intermediate complex [Ho·**11**] has been reported previously[3a] via the triester **10**, and was O-alkylated with 4-chloromethylphenylacetate in DMSO to yield the target ester, [Ho·L^4]. The synthesis of the phosphinate complex [Ln·L^5] followed a different route. Monoalkylation of cyclen in MeCN with the CF_3-labelled α-chloroamide, containing a *para*-ethyl ester group, yielded the secondary amine, **9**. Subsequent treatment with paraformaldehyde and $MeP(OEt)_2$ allowed the introduction of the phosphinate ester groups, through an Arbusov reaction. Base hydrolysis of the ester groups followed by complexation of the appropriate Ln ion in aqueous media gave the complexes [Ln·**13**], from which [Ln·L^5] was made by either O-alkylation or by a coupling reaction with 4-hydroxymethylacetanilide in DMF, mediated by HATU (Scheme 5). Final complexes were purified by reverse phase HPLC.

Calcium-selective probe behaviour: The complex [Gd·L^6] has been shown to exhibit a proton relaxivity that varies as a function of calcium concentration, with a dissociation constant of 450 μM in human serum solution (pH 7.4, 310 K).[8] The relaxivity increased by up to 67% on calcium binding (1.4 T, 310 K), as the hydration state of the complex switched from zero to one. This behaviour was shown to be independent of pH over the range 5.5 to 8 and was selective for Ca^{2+} over K^+, Na^+, Mg^{2+} and Zn^{2+} at equivalent concentrations, or at the values typically found for these cations in extracellular biological fluids. This selectivity profile is a property of the calcium-binding moiety, and should be re-

tained in the fluorinated analogue, [Ln·L^1]. Accordingly, prior to the NMR spectroscopy work with the Dy and Tm complexes, the performance of [Gd·L^1] was examined as a calcium-selective contrast agent, in comparison to [Gd·L^6].

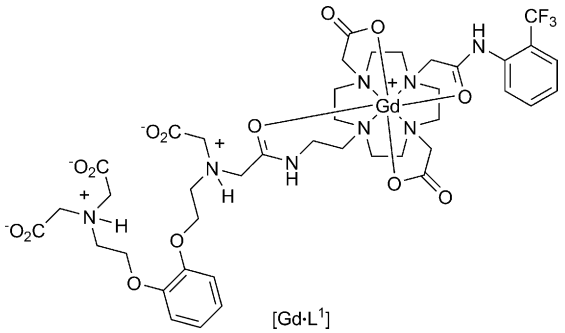

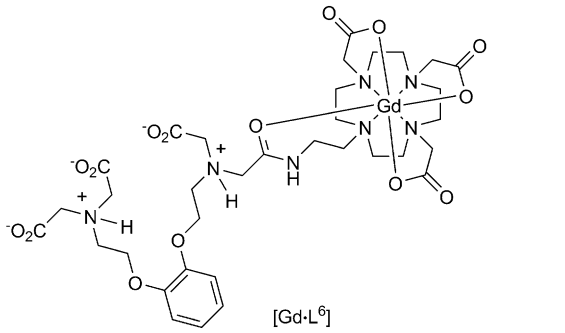

The proton relaxivity, r_{1p}, of [Gd·L^1] was 3.42 mM^{-1}s^{-1} (pH 7.2, 0.1 M MOPS, 310 K, 1.4 T) and increased to a limiting value of 6.62 mM^{-1}s^{-1} following addition of >1 equiv calcium chloride (Figure 1). By fitting the variation of the relaxivity with [Gd^{3+}] and assuming a 1:1 limiting stoichiometry, an estimate of the association constant was obtained by iterative fitting, with $\log K = 3.80(\pm 0.05)$ M^{-1}. This compares to a $\log K$ value of 3.59($\pm$0.03) M^{-1} for the calcium binding affinity of [Gd·L^6], measured under the same conditions. Less than a 6% change in proton relaxivity was observed in the presence of NaCl (110 mM), KCl (5 mM), $MgCl_2$ (1 mM) and $ZnCl_2$ (1 mM), consistent with the established selectivity profile. Subsequent addition of EDTA to the calcium-bound complex restored the initial relaxivity value, as the Ca^{2+} prefers to bind the added acyclic chelate. Such behaviour accords with the reversibility of calcium binding observed with [Gd·L^6].

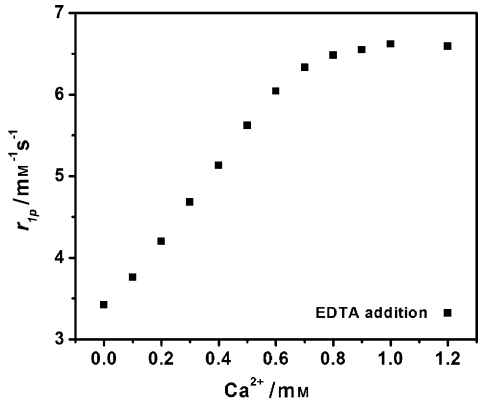

Figure 1. Variation of proton relaxivity with added Ca^{2+} and subsequent EDTA addition for an aqueous solution containing [Gd·L^1] (pH 7.2, 0.1 M MOPS, 310 K, 1.4 T, 1 mM complex) r_{1p} modulation = 94% (3.4 to 6.6 mM^{-1}s^{-1}).

Similar titration experiments were undertaken with [Dy·L^1] and [Tm·L^1], and the variation in the ^{19}F chemical shift of the trifluoromethyl group (4.7 T, 295 K, pH 7.2, 0.1 M MOPS) as a function of the calcium ion concentration was observed (Figure 2). With [Dy·L^1], addition of calcium was characterised by a shift of 3.0 ppm to higher frequency (−69 to −66 ppm), and for [Tm·L^1] the shift change was 3.9 ppm (−94.6 to −98.5 ppm) to lower frequency. The longitudinal relaxation rate, R_1, did not change by more than 4%, in each case, for the "free" and calcium-bound complexes. For example, with [Dy·L^1], R_1 was 169 Hz at 9.4 T and 100 Hz at 4.7 T and these values were 166 and 97 Hz, respectively, on adding calcium. The insensitivity of R_1 to added calcium indicates clearly that the CF_3 group remains at the same distance from the Ln ion. On the other hand, the observed

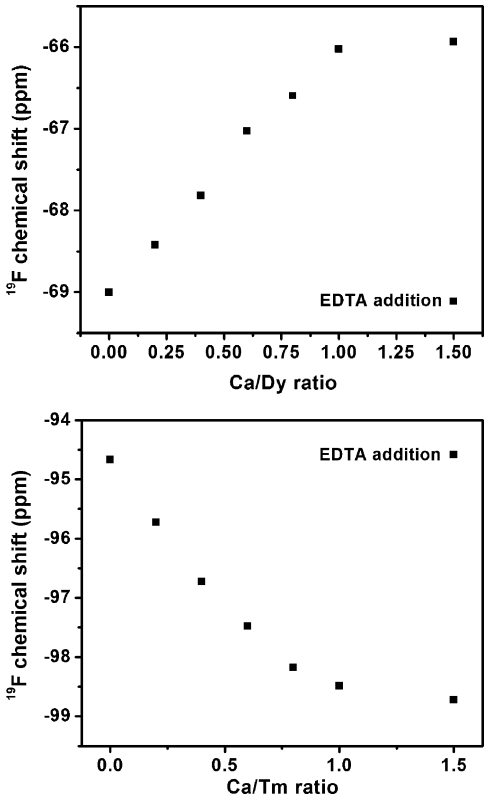

Figure 2. Variation of δ_F with added Ca^{2+} and subsequent EDTA addition for an aqueous solution containing, top: [Dy·L^1] (pH 7.2, 0.1 M MOPS, 295 K, 188 MHz, D_2O lock, 4 mM complex $\Delta\delta_F = 3$ ppm); bottom: [Tm·L^1] (as above, but 2 mM complex $\Delta\delta_F = 4$ ppm).

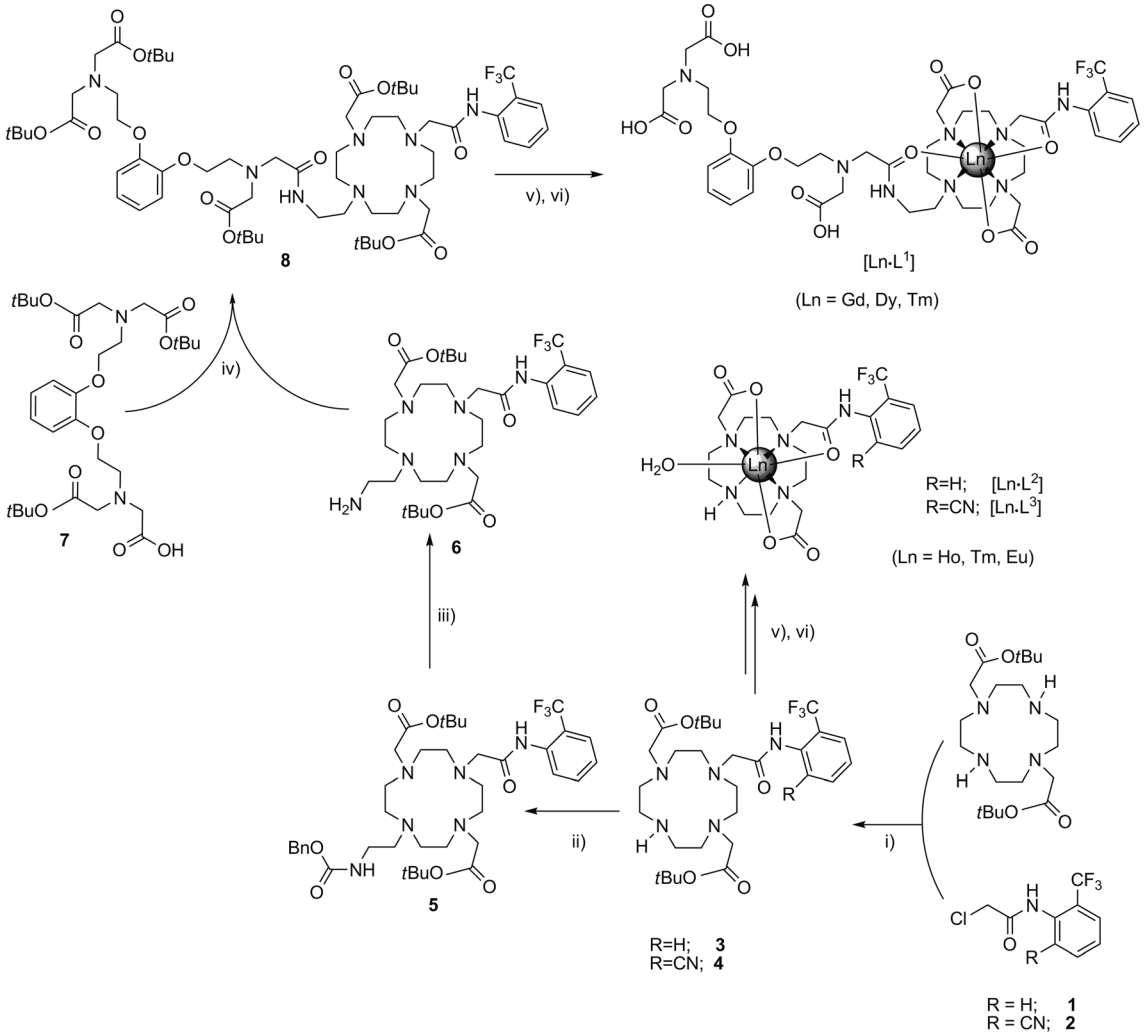

Scheme 4. Reagents and conditions: i) Na_2CO_3, anhydrous MeCN, 35–50%; ii) benzyl 2-bromoethylcarbamate, K_2CO_3, MeCN, 32%; iii) Pd-C (10%), H_2, MeOH, 40 psi, 65%; iv) NMM, EDC, HOBt, DMF, 20%; v) TFA/CH_2Cl_2 (9:1), 65% for L^1/80% for L^2/76% for L^3; vi) $LnCl_3{\cdot}6H_2O$, H_2O, 60°C, 18 h.

linewidth did vary differentially between the Dy and Tm systems, and in a manner that was field dependent (Table 1). Such behaviour is consistent with chemical exchange contributing to the broadening of the observed resonance, superimposed on the broadening ascribed to paramagnetic relaxation.

Table 1. NMR spectroscopic data[a] in the presence and absence of added metal ions (295 K, pH 7.2, 0.1 M MOPS, 2 mM complex, 2 equiv of stated metal ion as chloride salt).

Complex	Cation	δ_F [ppm]	Linewidth [Hz] 4.7 T	Linewidth [Hz] 9.4 T
[Dy·L^1]	none	−69.0	84	188
[Dy·L^1]	calcium	−66.0	110	282
[Dy·L^1]	magnesium[b]	−68.5	95	220
[Dy·L^1]	zinc[b]	−68.9	95	214
[Tm·L^1]	none	−94.6	38	44
[Tm·L^1]	calcium	−98.5	110	106

[a] For [Dy·L^1] R_1 values were 169 and 100 Hz at 9.4 and 4.7 T, respectively; for [Tm·L^1], corresponding R_1 values were 47 and 23 Hz. [b] On further addition of $CaCl_2$ (2 mM) to this sample, the observed shift was −66.0 ppm, consistent with selective Ca binding; no change was found in the presence of NaCl (0.1 M) and KCl (5 mM).

An attempt was made to fit the variation of δ_F with [Ca^{2+}] for [Tm·L^1], and a binding constant value of $\log K = 3.4(\pm 0.1)\,M^{-1}$ (295 K, pH 7.2, 0.1 M MOPS) was estimated. The slightly weaker binding of the thulium complex to Ca^{2+} can be attributed to the higher affinity of the labile amide carbonyl oxygen for the more charge dense Tm centre.

The binding curves in Figure 2 allow the ratio of free and calcium bound complex to be established, from the observed chemical shift value. Given the selectivity for calcium binding observed, noting that δ_F does not vary significantly with pH (over the range 6 to 8), and knowing the dissociation constant, K_d, measured in the medium of interest, the calcium concentration can be estimated directly. It is given as the product of the ratio of bound/free complex and K_d (Scheme 6).

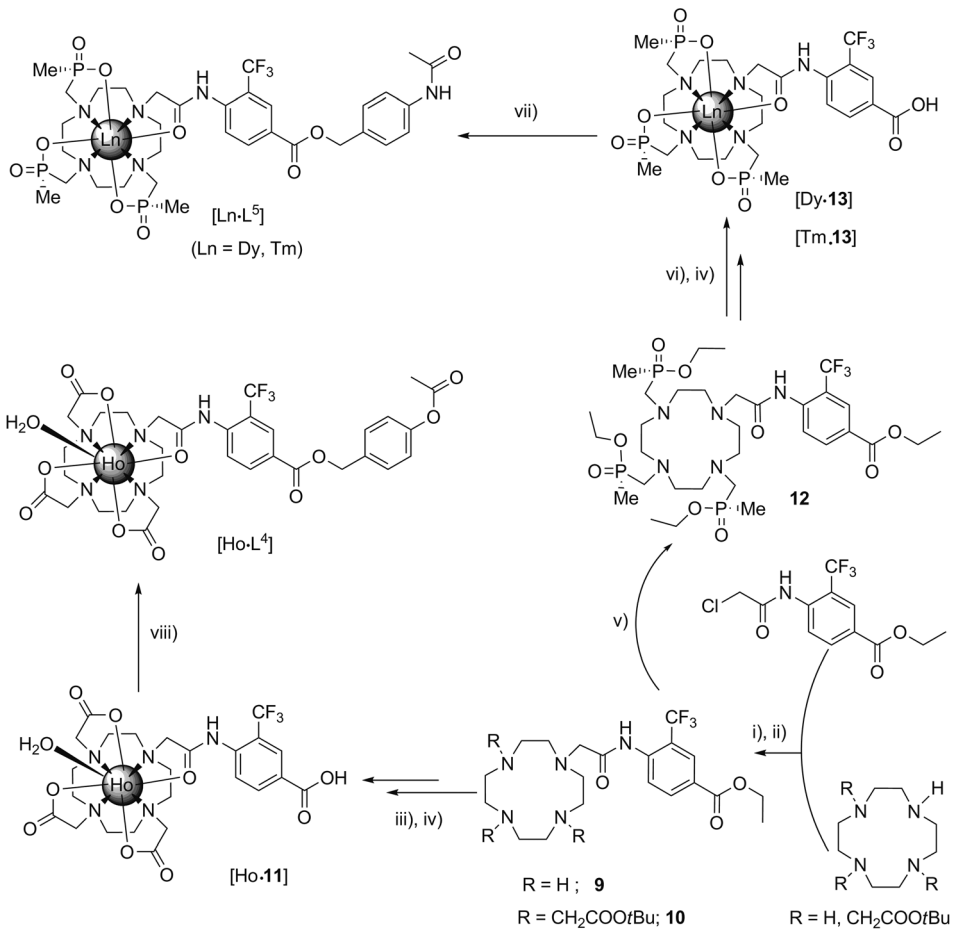

Scheme 5. Reagents and conditions: i) R = H: MeCN, 40 °C, 6 h, 64 % **9**; ii) R = CH_2CO_2tBu: MeCN, K_2CO_3, KI, reflux, 18 h, 78 % **10**; iii) 1) CH_2Cl_2/TFA (1:4), 24 h, 2) LiOH, 48 h, 77 %; iv) $LnCl_3{\cdot}6H_2O$, H_2O, 60 °C, 18 h; v) paraformaldehyde, diethylmethylphosphonite, THF, reflux, 18 h, 55 %; vi) KOD, 40 °C, 48 h, 40 %; vii) *N*-(4(hydroxymethyl)phenyl)acetamide, HATU, DIPEA, DMF, 48 h, 25 % [Dy·L^5] and *N*-(4-(chloromethyl)phenyl)acetamide/4-(chloromethyl)phenyl acetate, DMSO, K_2CO_3, 30 % [Tm·L^5]/[Ho·L^4].

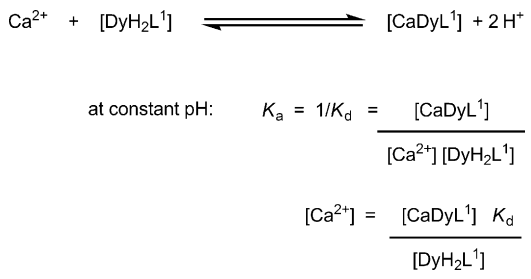

Scheme 6. Equilibrium associated with calcium binding.

Citrate selective chemical shift probe: When an anion binds to a lanthanide centre and displaces a coordinated water, the coordination change can be signalled by differences in the optical and NMR properties of the complex.[13d,18,19] With optical signal transduction, complexes of europium are frequently studied, as the emission spectra are most amenable to interpretation.

The Eu, Ho and Tm complexes of ligands L^2 and L^3 were prepared. In each case, the amide proton is relatively acidic and the pK_a was measured for each complex (Scheme 7), monitoring either variations in absorbance at 300 nm, or following changes in δ_F as a function of pH. The pK_a values (295 K, 0.1 M NaCl) were 7.24(±0.02) for [Ho·L^3], 6.57(±0.06) for [Eu·L^3] and 6.10(±0.04) for [Tm·L^3]. For the complexes of L^2, the corresponding pK_a values were all >8.5. For [Tm·L^3], the ^{19}F NMR spectroscopy and optical methods used to estimate the pK_a showed reasonable agreement (Figure 3).

Crystals of [Tm·L^3] were grown from aqueous solution and the X-ray structure was determined, revealing the geometry of the charge neutral conjugate base, that is, following deprotonation of the amide NH proton. The X-ray structure revealed several features. The single coordinated water molecule (Figure 4) is located 0.55 Å out of the plane defined by the other three coordinated oxygen atoms. The twist angle between the N4 and O4 planes is 38.4°, typical of related square antiprismatic complexes of lanthanide complexes with a coordination number of eight.[20] The trifluoromethyl group has a mean Tm–F distance of 6.48 Å, with

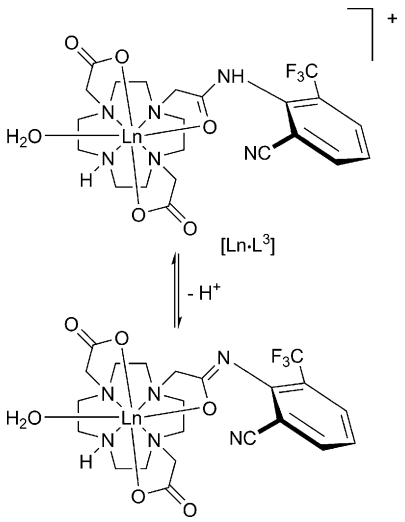

Scheme 7. Protonation equilibrium for [Ln·L^3].

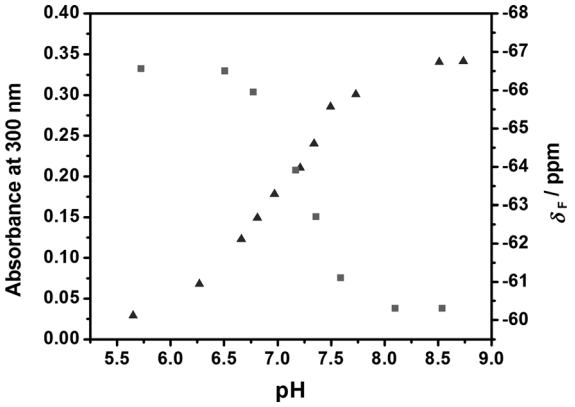

Figure 3. pH profiles for [Ho·L^3] observing absorbance intensity changes (λ_{abs} 300 nm; ▲) or variations in δ_F (■), associated with a pK_a of 7.15-(±0.1).

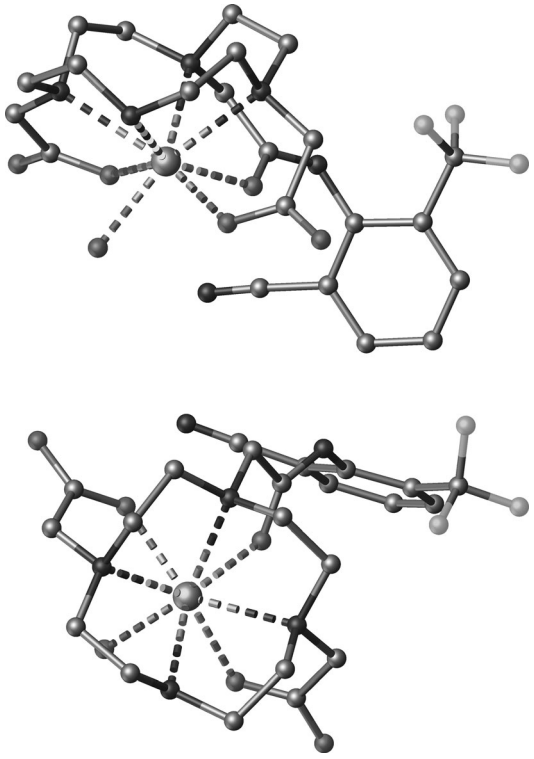

Figure 4. Views of the molecular structure of [Tm·L^3] from the X-ray analysis.

the individual fluorine atoms separated by distances of 5.34, 6.78 and 7.33 Å. The amide carbon–nitrogen bond is relatively short (1.30 Å) consistent with its double bond character. The nitrogen lone pair is able to conjugate effectively with the aromatic electrons, promoting the charge delocalisation into the *o*-cyano group that is associated with the absorption spectral change.

Before examining the ^{19}F NMR behaviour in solution, the anion affinities of the emissive Eu complex, [Eu·L^3(H$_2$O)$_2$] were established. Relative binding affinities were measured by examining the intensity ratio of the Eu $\Delta J=2$ to $\Delta J=1$ emission bands (see the Supporting Information) as a function of added anion concentration, by using reported methods[12,13] (Table 2). At pH 7.4, this system exhibits a modest selectivity for citrate. In a "fixed interference" background, containing the stated mixture of anions (Table 2, footnote), citrate was bound selectively with a reduced apparent affinity, associated with a K_d value of the order of 10 mM.

Table 2. Binding constants for [Eu·L^3] with selected anions, calculated from changes in the ratio of $\Delta J=2$ to $\Delta J=1$ bands of the emission spectrum (H$_2$O, pH 7.4, 50 mM HEPES, 2 mM complex, 0 to 100 mM [anion], 298 K, $\lambda_{exc}=397$ nm).

Anion	log K (±0.05)
citrate	2.71
lactate	1.98
phosphate	1.93
bicarbonate	0.81
citrate in anion mixture[a]	1.95

[a] Citrate competition experiment involved incremental addition of sodium citrate to a solution containing complex (2 mM), HEPES (50 mM), sodium bicarbonate (20 mM), sodium dihydrogenphosphate (1 mM), and sodium lactate (2 mM).

Changes in ^{19}F NMR parameters for the Ho and Tm complexes of L^2 and L^3 were monitored, following addition of up to a tenfold excess of the sodium salts of hydrogencarbonate, citrate, lactate and hydrogenphosphate at pD 7.4 in HEPES (50 mM) buffer (Table 3). At this pH, the aqua species of the complexes with L^2 gave rise to fairly sharp lines. In contrast, with [Ho·L^3], the observed resonance at −63.6 ppm was considerably broadened, associated with the chemical exchange between the protonated and deprotonated forms (pK_a ca. 7.15, Figure 3, vide supra). Exchange broadening was even more severe for [Tm·L^3], with a line-

Table 3. ^{19}F NMR spectroscopy data for [Ln·L^2] and [Ho·L^3] and their anion adducts (D$_2$O, 188 MHz, 295 K, pD 7.4, 2 mM complex, 50 mM HEPES, 10 equiv anion).

Complex	Anion	δ_F [ppm]:R_1(±3) [Hz]		Linewidth (±10) [Hz]
[Ho·L^2]	aqua species	−76.8	45	67
[Ho·L^2]	bicarbonate	~−66		broad[a]
[Ho·L^2]	lactate	−64.6		214
[Ho·L^2]	phosphate	−53.6		230
[Ho·L^2]	citrate	−66.5	48	208
[Tm·L^2]	aqua species	−67.6	23	120
[Tm·L^2]	bicarbonate	−63.2		189
[Tm·L^2]	lactate	−70.2		99
[Tm·L^2]	phosphate	−83.0		198
[Tm·L^2]	citrate	−72.3	25	175[b]
[Ho·L^3][c]	aqua species	−66.3	83	420
[Ho·L^3]	bicarbonate	−64.6		400
[Ho·L^3]	lactate	−68.6		1200
[Ho·L^3]	phosphate	−64.8		700
[Ho·L^3]	citrate	−68.0	91	260
[Ho·L^3]	mixture[d]	−68.1	92	250

[a] Linewidth >1500 Hz; [b] slow decomplexation of the Ln ion from the ligand was observed; [c] with [Tm·L^3], only addition of citrate gave rise to an observable signal at pD 7.4, $\delta_F=-61.1$ ppm, ($\omega_{1/2}=134$ Hz, $R_1=54$ Hz (295 K, 4.7 T) and $R_1=64$ Hz (9.4 T, 295 K); [d] mixture consists of 10 equiv each of phosphate, bicarbonate, lactate, and citrate.

width of >1500 Hz at 4.7 T and pD 7.4, such that the ^{19}F resonance was barely discernible. Lowering the pH sharpened the resonance for the aqua species, and at pD 4 it was observed at −61.4 ppm, with an R_1 value of 67 Hz at 9.4 T. At a given field, the R_1 values for the complexes of L^2 were significantly slower than those with L^3. For example, R_1 values for $[Ho{\cdot}L^2(H_2O)]$ and $[Ho{\cdot}L^3(H_2O)]$ at 4.7 T were 45 and 83 Hz, respectively. Given the r^{-6} dependence of R_1, arising from the electron–nuclear dipolar interaction, and noting the separation found in the X-ray analysis of $[Tm{\cdot}L^3(H_2O)]$, it can be estimated that the CF_3 group is about 0.6 Å closer to the metal ion in complexes of L^3.

Anion addition gave rise to shifted resonances with a characteristic ^{19}F chemical shift for each ternary adduct, associated with the change in the local ligand field at the Ln ion. Shift non-equivalence was greatest for adducts with the complexes of L^2. However, in equimolar mixtures of anions, no significant preference for binding to a given anion was observed. In these cases, single resonances with additional line-broadening were observed, associated with chemical exchange between free and bound anion adducts that is fast on the NMR timescale. With $[Ho{\cdot}L^3]$, anion addition gave rise to exchange broadened resonances at characteristic chemical shifts, and with added citrate, resonances were sharpest. Chemical shift values for the lactate and citrate ternary adducts were most similar, consistent with their known common coordination to an Ln centre, involving chelation of the α-hydroxy and carboxylate groups, verified in related crystallographic analyses of Yb, Eu and Ho complexes.[22]

In an equimolar mixture containing $[Ho{\cdot}L^3]$ and 10 equiv of each of the studied anions, only the citrate peak was observed (Table 3). This behaviour accords with the selectivity observed for $[Eu{\cdot}L^3]$ defined above (Table 2). Incremental addition of citrate to $[Ho{\cdot}L^3]$ allowed free and bound species to be observed simultaneously by ^{19}F NMR spectroscopy (see the Supporting Information). Following addition of 0.5 equiv citrate, each species was present in approximately 50:50 ratio, consistent with chemical exchange between the aqua species and the citrate adduct that is slow on the NMR timescale.

With $[Tm{\cdot}L^3(H_2O)]$, only addition of citrate gave rise to a resonance that was not severely broadened by chemical exchange. Selectivity for citrate was again noted in equimolar anion mixtures. Incremental addition of citrate at pD 7.4 was monitored by ^{19}F NMR spectroscopy, with trifluoroethanol as an internal reference to allow the change in intensity of the emerging bound citrate signal to be followed (see the Supporting Information and Figure 5). The apparent affinity constant measured ($\log K = 2.79(\pm 0.03)\,M^{-1}$), corresponds well to that defined for $[Eu{\cdot}L^3]$, monitoring emission spectral changes (Table 2).

Signalling a remote functional group transformation: The diester, $[Ho{\cdot}L^4(H_2O)]$, gives rise to one major solution species ($\delta_F = -50.8$ ppm). It contains a remote phenolic ester group that following hydrolysis was envisaged to trigger

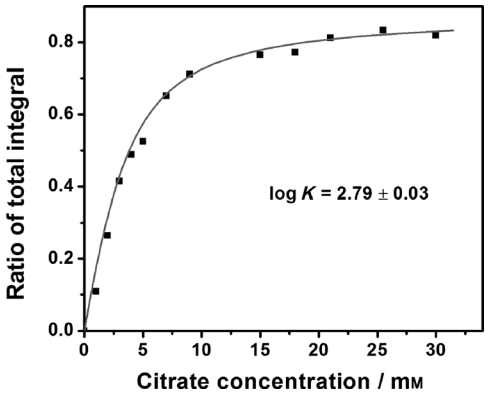

Figure 5. Binding curve for addition of citrate to $[Tm{\cdot}L^3(H_2O)]$, showing the fit (line) to the experimental data, following the increase in relative intensity of the $[Tm{\cdot}L^3(citrate)]$ signal at −61.1 ppm, reported as the ratio of the total signal area with respect to added trifluoroethanol at −77.3 ppm (298 K, 188 MHz, 3 mM complex, D_2O, pD 7.4, 0.2 mM CF_3CH_2OH).

cleavage of the aryl-carboxylate ester, in a stepwise manner, based on the "self-immolative" property of these systems[16,17] (Scheme 8). The product carboxylate complex, gives rise to a single resonance at −57 ppm ($\Delta\delta_F = 6.2$ ppm, 295 K, pH 7.4). Following addition of either pig-liver esterase or α-chymotrypsin to solutions containing the ester, under standard conditions, the ^{19}F NMR spectrum was monitored as a function of time. Little change in the NMR spectrum was observed over a period of 24 h. Analysis by LCMS revealed the build-up of a new peak at *m/z* 868 (negative ion ESMS), consistent with formation of the intermediate

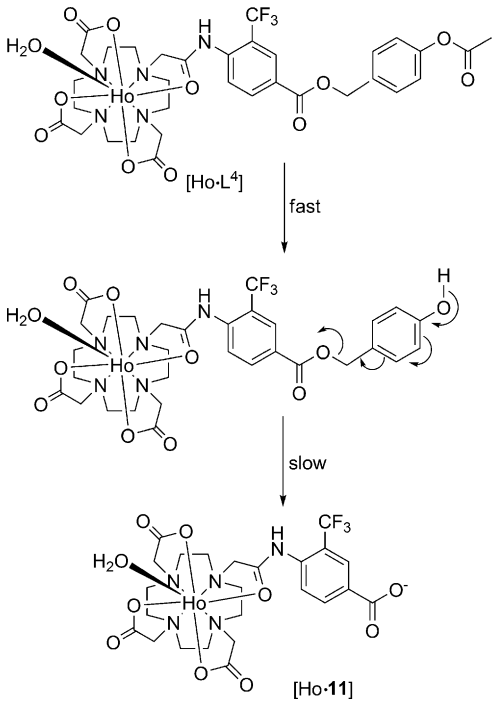

Scheme 8. Stepwise cleavage of $[Ho{\cdot}L^4]$ induced by added pig-liver esterase or α-chymotrypsin (pH 7.4, 310 K).

phenol. In control experiments at elevated pH, this intermediate underwent further hydrolysis at ambient temperature only at pH 10. In a further control experiment, the enzymatic hydrolysis of the ethyl ester of [Ho·**11**] was examined, under the same conditions. Slow catalysis of ester hydrolysis was observed by using pig-liver esterase, but the reaction only proceeded to 50% conversion. In each case product inhibition of enzyme activity might suppress the cleavage reaction.

The lanthanide complexes of L^4 give rise to several isomers in solution,[4a] but for the corresponding triphosphinate series, only one isomer is favoured in solution (>85% typically). Furthermore, as the intermediate phenolate had not cleaved as rapidly as had been envisaged, the related amide system, [Ln·L^5] was examined. In the presence of α-chymotrypsin, changes in the ^{19}F NMR spectrum of [Ln·L^5] (Ln = Dy and Tm) were followed as a function of time (Figure 6).

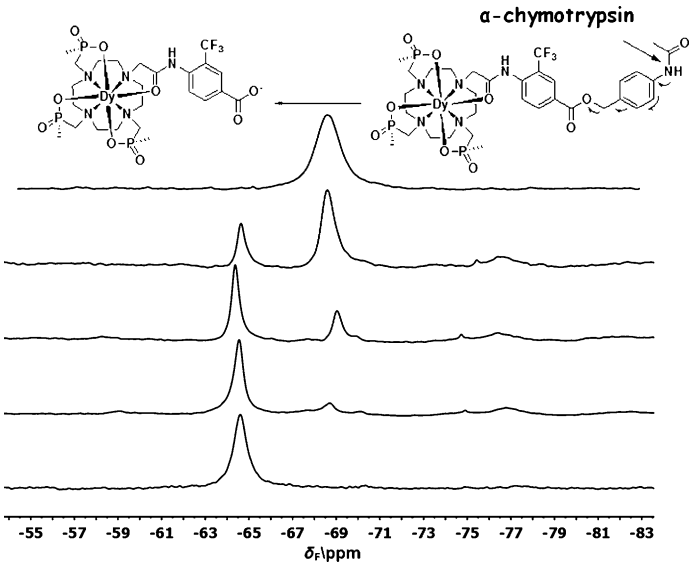

Figure 6. Changes in the ^{19}F NMR spectrum of [Dy·L^5], following cleavage of the remote amide bond induced by α-chymotrypsin (pH 7.4, 9.4 T, 295 K; spectra shown above were measured at pH 6.5; substrate at top, product at bottom).

The ^{19}F shift non-equivalence between [Dy·L^5] and the product carboxylate complex was 4.8 ppm, and for [Tm·L^5], $\Delta\delta_F$ was 12.1 ppm. Thus, the cleavage reaction could be monitored easily. The greater linewidth of the precursor amide is caused by chemical exchange with the conjugate base, associated with its lower pK_a, as noted in related earlier work.[2b,3a] Therefore, during acquisition of the spectral data, the pH was temporarily lowered to 6.5. A feature of these systems was their sluggishness, taking about 10 days to reach completion, as found with [Ho·L^4]. Evidently, although these systems are not good substrates for the esterase and protease examined, the facility of following changes in the hydrolysis reaction directly by ^{19}F NMR spectroscopy opens up possibilities for directly monitoring such hydrolytic cleavage reactions in situ with spatial resolution, by using chemical shift imaging.

Conclusion

With these three diverse examples, we have demonstrated how amplified shift non-equivalence, coupled with faster signal acquisition arising from enhanced rates of longitudinal relaxation, can be combined to devise paramagnetic probes that allow monitoring of both reversible and irreversible reactions by ^{19}F NMR spectroscopy.

Modulation of calcium concentration in the millimolar range has been shown to cause changes in the relative concentration of free and bound Ca^{2+} at the remote engineered binding site in [Ln·L^1]. This event triggers a reversible change in the lanthanide coordination environment that modulates the pseudo-contact shift, amplifying the chemical shift non-equivalence of the CF_3 reporter group. The "pyro-EGTA" Ca^{2+} binding moiety used, has been shown to possess good selectivity for calcium over sodium, magnesium and zinc at the concentration levels of each "free" ion likely to be present in biological samples.[8] Here, this behaviour is also shown to be in agreement with the findings for the analogous Gd system, in which water proton relaxivity is modulated reversibly and selectively, because of a change in metal hydration state.

Reversible anion binding in aqueous solution at a lanthanide centre also changes the dipolar shift of ligand resonances, by altering the second-order crystal field coefficient, B_2^0, that is a function of the local coordination environment. Here, we have established proof-of-principle using a monocationic complex containing a reporter CF_3 group, to show that chemoselective binding of citrate can be signalled by a change in δ_F. Citrate selectivity is also demonstrated for the related Eu complex, by using emission spectral changes to allow quantification of anion binding constants.

Finally, building on earlier work of Mason,[1a,6a] we demonstrate that ester cleavage can be signalled by a ^{19}F shift change using a CF_3 reporter, with which the observed non-equivalence can be amplified to 12 ppm, an order of magnitude greater than shift differences typically found with diamagnetic systems.[23]

Experimental Section

Details of instrumentation, ligand synthesis, methods of purification, characterisation, relaxivity measurements and spectral titrations are given in the Supporting Information.

General preparation of lanthanide complexes of L^1: Lanthanide complexes of L^1 were prepared from corresponding solutions of the ligand (1 equiv) and solutions of $GdCl_3·6H_2O$/$DyCl_3·6H_2O$ or $TmCl_3·6H_2O$ (1.5 equiv). The reaction mixture was stirred at 80°C for 20 h. The pH was periodically checked and adjusted to 6.5 by using solutions of NaOH (1 M) and HCl (1 N) as needed. After completion, the reaction mixture was cooled and passed through Chelex-100 to trap free or weakly bound Ln^{3+} ions, and the Ln-loaded complexes were eluted. The fractions were dialyzed (500 MW cut off; Spectra/Pro® biotech cellulose ester dialysis membrane, Spectrum Laboratories), purified by semi-preparative RP-HPLC and lyophilized to obtain off-white solids. These complexes were characterized by ESI-MS in positive and negative mode and the appro-

priate isotope pattern distributions for $Gd^{3+}/Dy^{3+}/Tm^{3+}$ were recorded (see the Supporting Information).

[Gd·L^1]: Yield = 3 mg (off white solid), 52%; ESI-MS (+): calcd $C_{41}H_{55}F_3{}^{155}GdN_8O_{14}$: *m/z* 1096.3 $[M+H]^+$; found 1096.4 $[M+H]^+$, r_{1p} (1.4 T, pH 7.2) = 3.42 [$mM^{-1}s^{-1}$]; HPLC, t_R = 5.34 min.

[Dy·L^1]: Yield = 2.6 mg (off white solid), 45%; ^{19}F NMR (376 MHz, H_2O, pH 7.2): $\delta = -69.0$ ppm; ESI-MS (+): calcd $C_{41}H_{55}{}^{160}DyF_3N_8O_{14}$: *m/z* 1101.3 $[M+H]^+$; found 1101.3 $[M+H]^+$, HPLC, t_R = 5.31 min.

[Tm·L^1]: Yield = 2.2 mg (off white solid), 38%; ^{19}F NMR (376 MHz, H_2O, pH 7.2): $\delta = -94.6$ ppm; ESI-MS (+): calcd $C_{41}H_{55}F_3N_8O_{14}{}^{169}Tm$: *m/z* 1110.3 $[M+H]^+$; found 1110.3 $[M+H]^+$, HPLC, t_R = 5.32 min.

X-ray crystallography: The single crystal X-ray data for [Tm·L^3] were collected at 120 K on a Gemini Ultra (Agilent Technologies) diffractometer (graphite monochromator, $\mu(Mo_{K\alpha})$, $\lambda = 0.71073$ Å) equipped with Cryostream (Oxford Cryosystems) open-flow nitrogen cryostat. Using Olex2[23] software, the structure was solved with the XS[24] structure solution program by Patterson methods and refined with the XL[25] refinement package with full-matrix least squares minimisation. All hydrogen atoms were placed in calculated positions and refined in riding mode, disordered atoms were refined isotropically with fixed SOF = 0.5. CCDC 870354 contains the supplementary crystallographic data for this paper. These data can be obtained free of charge from The Cambridge Crystallographic Data Centre via www.ccdc.cam.ac.uk/data_request/cif.

Crystal data for [Tm·L^3]: $C_{22}H_{37}F_3N_6O_{10}Tm$, $M_r = 771.51$, monoclinic, $a = 7.55031(18)$, $b = 32.7541(7)$, $c = 11.8075(3)$ Å, $\beta = 101.046(2)°$, $V = 2865.93(11)$ Å^3, space group $P2_1/c$, $Z = 4$, $\mu(Mo_{K\alpha}) = 3.178$, 20173 reflections measured, 7618 unique ($R_{int} = 0.0659$), which were used in all calculations. The final wR_2 was 0.1016 (all data) and R_1 was 0.0604 for 5270 reflections with $I > 2\sigma(I)$, GOF = 1.085.

Acknowledgements

We thank EPSRC, CRC-UK and the ERC (FCC266804) for support, and Dr. Dmitry Yufit for the crystallographic analysis of [Tm·L^3].

[1] a) Y. Yu, V. D. Kodibagkar, W. Cui, R. P. Mason, *Curr. Med. Chem.* **2005**, *12*, 819; b) M. A. Danielson, J. J. Falke, *Annu. Rev. Biophys. Biomol. Struct.* **1996**, *25*, 163; c) C. Belle, C. Beguin, S. Hamman, J.-L. Pierre, *Coord. Chem. Rev.* **2009**, *253*, 963; d) G. A. Smith, R. T. Hesketh, J. C. Metcalfe, J. Feeney, P. G. Morris, *Proc. Natl. Acad. Sci. USA* **1983**, *80*, 7178.

[2] a) P. K. Senanayake, A. M. Kenwright, D. Parker, S. van der Hoorn, *Chem. Commun.* **2007**, 2923; b) A. M. Kenwright, I. Kuprov, E. De Luca, D. Parker, S. U. Pandya, P. K. Senanayake, D. G. Smith, *Chem. Commun.* **2008**, 2514.

[3] a) K. H. Chalmers, E. De Luca, N. H. M. Hogg, A. M. Kenwright, I. Kuprov, D. Parker, M. Botta, J. I. Wilson, A. M. Blamire, *Chem. Eur. J.* **2010**, *16*, 134; b) P. Harvey, I. Kuprov, D. Parker, *Eur. J. Inorg. Chem.* **2012**, 2015.

[4] a) K. H. Chalmers, M. Botta, D. Parker, *Dalton Trans.* **2011**, *40*, 904; b) K. H. Chalmers, A. M. Kenwright, D. Parker, A. M. Blamire, *Magn. Reson. Med.* **2011**, *66*, 931; c) F. Schmid, C. Holtke, D. Parker, C. Faber, *Magnet. Reson. Med.* in press, DOI: 10.1002/mrm.24341; d) Z.-X. Jiang, Y. Feng, Y. B. Yu, *Chem. Commun.* **2011**, *47*, 7233.

[5] a) I. D. Stegman, A. Rehemtulla, B. Beattie, A. Kievit, T. S. Lawrence, R. G. Blasberg, J. G. Tjuvajev, B. D. Ross, *Proc. Natl. Acad. Sci. USA* **1999**, *96*, 9821; b) W. E. Hull, R. E. Port, R. Hermann, B. Britsch, W. Kunz, *Cancer Res.* **1988**, *48*, 1680; c) S. L. Cobb, C. D. Murphy, *J. Fluorine Chem.* **2009**, *130*, 132; d) D. G. Reid, P. S. Murphy, *Drug Discovery Today* **2008**, *13*, 473.

[6] a) V. D. Kodibagkar, J. Yu, Y. Liu, H. P. Hetherington, R. P. Mason, *Magn. Reson. Imaging* **2006**, *24*, 959; b) S. Mizukami, R. Takikawa, F. Sugihara, Y. Hori, H. Tochio, M. Walchli, M. Shirakawa, K. Kikuchi, *J. Am. Chem. Soc.* **2008**, *130*, 794; c) C. Dalvit, N. Mangelli, G. Papeo, P. Giordano, M. Veronesi, D. Moskau, R. Kummerle, *J. Am. Chem. Soc.* **2005**, *127*, 13380; d) E. Papeo, P. Giordano, M. G. Brasca, F. Buzzo, D. Carroni, F. Ciprandi, N. Mangelli, M. Veronesi, A. Vulpetti, C. Dalvit, *J. Am. Chem. Soc.* **2007**, *129*, 5665; e) S. Mizukami, H. Matsushita, R. Takikawa, F. Sugihara, M. Shirakawa, K. Kikuchi, *Chem. Sci.* **2011**, *2*, 1151; f) S. Mizukami, *Chem. Pharm. Bull.* **2011**, *59*, 1435.

[7] B. Bleaney, *J. Magn. Reson.* **1972**, *8*, 91.

[8] A. Mishra, N. K. Logothetis, D. Parker, *Chem. Eur. J.* **2011**, *17*, 1529.

[9] a) M. P. Lowe, D. Parker, O. Reany, S. Aime, M. Botta, E. Castellano, E. Gianolio, *J. Am. Chem. Soc.* **2001**, *123*, 7601; b) M. P. Lowe, D. Parker, *Chem. Commun.* **2000**, 707; c) S. Aime, M. Botta, J. A. K. Howard, R. Kataky, M. P. Lowe, J. M. Moloney, D. Parker, A. S. de Sousa, *Chem. Commun.* **1999**, 2415.

[10] a) K. Dhingra, M. E. Maier, M. Beyerlin, G. Angelovski, N. K. Logothetis, *Chem. Commun.* **2008**, 3444; b) J. L. Major, R. M. Boiteau, T. J. Meade, *Inorg. Chem.* **2008**, *47*, 10788.

[11] A. Congreve, D. Parker, E. Gianolio, M. Botta, *Dalton Trans.* **2004**, 1441.

[12] a) D. Parker, J. Yu, *Chem. Commun.* **2005**, 3141; b) J. Yu, R. Pal, D. Parker, R. Poole, M. J. Cann, *J. Am. Chem. Soc.* **2006**, *128*, 2294.

[13] a) R. Pal, L. C. Costello, D. Parker, *Org. Biomol. Chem.* **2009**, *7*, 1525; b) D. Parker, *Chem. Soc. Rev.* **2004**, *33*, 156.

[14] R. Pal, A. Beeby, D. Parker, *J. Pharm. Biomed. Anal.* **2011**, *56*, 352.

[15] C. P. Montgomery, E. J. New, R. Pal, D. Parker, *Acc. Chem. Res.* **2009**, *42*, 925.

[16] a) Y. Meyer, J. A. Richard, B. Delest, P. Noack, P. Y. Renard, A. Romieu, *Org. Biomol. Chem.* **2010**, *8*, 1777; b) H. Y. Lee, X. Jiang, D. W. Lee, *Org. Lett.* **2009**, *11*, 2005.

[17] a) K. Abu Ajaj, M. L. Biniossek, F. Kratz, *Bioconjugate Chem.* **2009**, *20*, 390; b) J. A. Duimstra, F. J. Femia, T. J. Meade, *J. Am. Chem. Soc.* **2005**, *127*, 12847.

[18] J. I. Bruce, R. S. Dickins, D. Parker, D. J. Tozer, *Dalton Trans.* **2003**, 1264.

[19] a) L. De Bari, D. Parker, G. Pintacuda, R. S. Dickins, P. Salvadori, *J. Am. Chem. Soc.* **2000**, *122*, 9257; b) P. Atkinson, Y. Bretonniere, D. Parker, *Chem. Commun.* **2004**, 438; c) Y. Bretonniere, M. J. Cann, D. Parker, R. Slater, *Org. Biomol. Chem.* **2004**, *2*, 1624.

[20] a) D. Parker, R. S. Dickins, H. Puschmann, C. Crossland, J. A. K. Howard, *Chem. Rev.* **2002**, *102*, 1977; b) P. Caravan, J. J. Ellison, T. J. McMurry, R. B. Lauffer, *Chem. Rev.* **1999**, *99*, 2293.

[21] a) E. Terreno, M. Botta, P. Boniforte, C. Bracco, L. Milone, B. Mondino, F. Uggeri, S. Aime, *Chem. Eur. J.* **2005**, *11*, 5531; b) E. Terreno, M. Botta, W. Dastru, S. Aime, *Contrast Media Mol. Imaging* **2006**, *1*, 101.

[22] R. S. Dickins, J. A. K. Howard, A. S. Batsanov, M. Botta, J. I. Bruce, C. S. Love, D. Parker, R. D. Peacock, H. Puschmann, *J. Am. Chem. Soc.* **2002**, *124*, 12697.

[23] J. Yu, L. Liu, V. D. Kodibagkar, W. Cui, R. P. Mason, *Bioorg. Med. Chem.* **2006**, *14*, 326.

[24] O. V. Dolomanov, L. J. Bourhis, R. J. Gildea, J. A. K. Howard, H. Puschmann, *J. Appl. Crystallogr.* **2009**, *42*, 339.

[25] G. M. Sheldrick, *Acta Crystallogr. A* **2008**, *64*, 112.

Received: April 4, 2012
Published online: ■■ ■■, 2012

A change of scenery: Variations in the coordination environment of paramagnetic lanthanide complexes are signalled by changes in the chemical shift of a reporter CF_3 group. Examples include reversible calcium (shown in structure) or citrate binding in the mM range, as well as the irreversible hydrolysis of a remote amide or ester group.

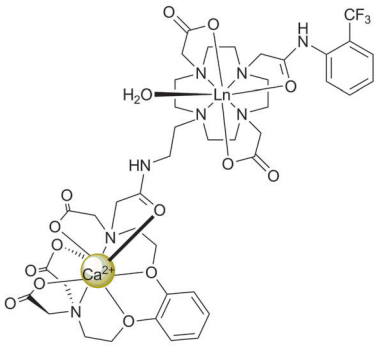

Lanthanides

P. Harvey, K. H. Chalmers, E. De Luca, A. Mishra, D. Parker** ..... ▮▮▮▮–▮▮▮▮

Paramagnetic ^{19}F Chemical Shift Probes that Respond Selectively to Calcium or Citrate Levels and Signal Ester Hydrolysis